A new methodology for measuring traveling quasi-5-day oscillations during SSWs based on satellite observations

Zheng Ma[1, 2], Yun Gong[1, 2], Shaodong Zhang[1, 2, 3, 4], Qiao Xiao[1, 2], Chunming Huang[1, 2], and Kaiming Huang[1, 2]

1. School of Electronic Information, Wuhan University, Wuhan, China.
2. Key Laboratory of Geospace Environment and Geodesy, Ministry of Education, Wuhan, China.
3. State Key Laboratory of Information Engineering in Surveying, Mapping and Remote Sensing, Wuhan University, Wuhan, China.
4. Guizhou Normal University, Guiyang, China.

Correspondence to Yun Gong (yun.gong@whu.edu.cn)

Abstract

Enhancements of stationary planetary waves (SPWs) and traveling planetary waves (TPWs) are commonly observed in the middle atmosphere during sudden stratospheric warming (SSW) events. Based on the least--square fitting method (Wu et al., 1995), numerous studies have used satellite measurements to investigate the characteristics of TPWs during SSWs but ignored the effect of the SPWs. However, a rapid and large change in the SPWs during SSWs may lead to significant disturbances in the amplitude of derived TPWs. In this study, we present a new methodology for obtaining the amplitudes and wavenumbers of traveling quasi-5-day oscillations (Q5DOs) in the middle atmosphere during major SSWs. Our new fitting method is developed by inhibiting the effect of a rapid and large change in SPWs during SSWs. We demonstrate the effectiveness of the new method using both synthetic data and satellite observations. The results of the simulations indicate that the new method can suppress the aliasing from SPWs and capture the real variations of TPWs during SSWs. Based on the geopotential height data measured by the Aura satellite from 2004 to 2021, the variations of traveling Q5DOs during eight mid-winter major SSWs are reevaluated using the new method. The differences in the fitted amplitudes between the least--square fitting method and the new method are usually over 100 m during the SSW onsets. Our analysis indicates that previously-reported Q5DOs during SSWs might be contaminated by SPWs, which leads to both overestimation and underestimation in the amplitudes of the traveling Q5DOs.

1. Introduction

Sudden stratospheric warming (SSW) is one of the most representative phenomena in the atmospheric dynamics in the polar region, which is excited by the interaction between stationary planetary waves (SPWs) and background mean flow (Matsuno, 1971; Baldwin et al., ~~2020~~2021). The onset of SSW is characterized by a positive ~~temperature~~ gradient of zonal mean temperature between 90°N and 60°N at 10 hPa (Andrews et al., 1987). Generally, a major SSW event is additionally associated with the phenomenon of wind reversals in the zonal mean eastward winds at 60°N and 10 hPa; otherwise, SSWs are regarded as minor events (Charlton and Polvani, 2007; Butler et al., 2017; Choi et al., 2019). During the occurrence of SSWs, the enhancements of SPWs largely affect the energy transportation in the stratosphere and the occurrence of extreme weather in the troposphere at middle latitudes (e.g., Manney et al., 2009; Kozubek et al., 2015; King et al., 2019; Domeisen et al., 2020). The zonal wavenumber of the enhanced SPWs usually corresponds to the geometry of the polar vortex during SSWs (e.g., Harada and Hirooka, 2017; Liu et al., 2019; White et al., 2021). A displacement vortex is mainly due to a strong SPW with a zonal wavenumber of 1 (SPW1) and split vortices are always associated with large SPWs with a zonal wavenumber of 2 (SPW2) (e.g., Seviour et al., 2013; Lawrence and Manney, 2018; Choi et al., 2019).

Traveling planetary waves (TPWs), widely observed with strong amplitudes during SSWs in recent decades, also play a significant role in controlling the global atmospheric and ionospheric couplings during SSWs (e.g., Gong et al., 2019; Koushik et al., 2020; Lin et al., 2020; Ma et al., 2022). One of the prominent TPWs, the westward propagating quasi-5-day oscillation (Q5DO) with periods of 4-7 days, is usually observed from the mesosphere to the ionosphere at mid-latitudes during SSWs with the zonal wavenumbers both 1 and 2 (W1 and W2) (Gong et al., 2018; Pancheva et al., 2018; Yamazaki et al., 2020, 2021). These Q5DOs are believed to be generated by atmospheric barotropic/baroclinic instability due to large changes in zonal winds and temperatures during SSWs (e.g., Liu et al., 2004; Ma et al., 2020; Yamazaki et al., 2021). Based on the least-square fitting method introduced by Wu et al. (1995), the amplitude, phase, and zonal wavenumber of the Q5DOs can be obtained from satellite observations and reanalysis data sets (e.g., Huang et al., 2017; Qin et al., 2021). However, based on the least-square fitting method, a rapid and large change in the amplitudes of SPWs would lead to an apparent fluctuation in the amplitude of TPWs over a broad range of frequencies, including those corresponding to Q5DOs. Yamazaki and Matthias (2019) proposed that based on the least-square fitting method, the effect of an SPW on a quasi-10-day wave (Q10DW) is equivalent to two oppositely propagating waves with equal amplitudes, periods, and wavenumbers. They suggested that the effect of SPWs can be ignored when the activities of Q10DWs in the oppositely propagating direction were not simultaneously enhanced.

However, the rapid change in the amplitudes of SPWs is a typical characteristic during the occurrence of SSWs. Previous studies usually ignored the effect of SPWs when obtaining the amplitudes of Q5DOs from satellite observations (e.g., Gong et al., 2018; Qin et al., 2021). Nevertheless, both westward and eastward Q5DOs have been frequently reported during SSWs in recent years (e.g., Pancheva et al., 2018; Rhodes et al., 2021; Wang et al., 2021; Yu et al., 2022). Thus, it is necessary to understand the real physics of the enhanced Q5DOs during SSWs and their relationships with SPWs. It is also necessary to inhibit the effect of SPWs when studying the variations of Q5DOs during SSWs. In the present study, we develop a new method for measuring the variation of westward and eastward propagating Q5DOs by inhibiting the effect of a rapid and large change in SPWs. The effectiveness of the new method is demonstrated by using both simulations and satellite observations. The paper is organized as follows. In Section 2, the synthetic data and the satellite data used in this study are introduced. Section 3 presents the new methodology for measuring the amplitudes of Q5DOs. Discussions are given in Section 4, mainly focusing on the comparisons of traveling Q5DOs during SSWs between the least-square fitting method and the new fitting method. Conclusions are summarized in section 5.

2. Data

In the present study, a simulation is performed based on synthetic data to further understand the issue of SPWs and Q5DOs during SSWs. The synthetic data $\mathrm{Y}(x,t)$ are built based on equation (1), including three components: an SPW, a westward propagating Q5DO, and an eastward propagating Q5DO, respectively, which is expressed as:

$$\mathrm{Y}(x,t) = A_k(t)\cos(kx-\varphi_k) + B_w\cos(\omega t + kx - \varphi_w) + B_e\cos(\omega t - kx - \varphi_e) \quad (1)$$

where x is the longitudes, t is the time, k is the wavenumber, ω is the frequency of

Q5DOs, A_k and φ_k are the amplitude and phase of SPWs, B_w and B_e denote the amplitudes of westward and eastward Q5DOs with the phase of φ_w and φ_e, respectively. Based on the least least-square fitting method introduced by Wu et al. (1995), TPWs with the same zonal wavenumber but in other periods only cause periodic modulation in the fitted amplitudes of Q5DOs. The aliasing caused by TPWs with different wavenumbers is mainly captured in the studies of quasi-2-day waves based on satellite measurements (Tunbridge et al., 2011). For the analysis of Q5DOs, the aliasing caused by TPWs with different wavenumbers is usually ignored, because Q5DOs with wavenumbers of 3 or 4 are rarely reported. Nevertheless, the most important issue of the least--square fitting method may be the aliasing due to the rapid and large changes in the SPWs. Therefore, to better understand the issue, the synthetic data for the simulations in the present study only includes three components of waves with the same zonal wavenumbers.

To verify the effectiveness of different fitting methods, the geopotential height data measured by the Aura/Microwave Limb Sounder (MLS) from 2005 to 2021 are used to derive the Q5DOs in the present study. The available Aura/MLS geopotential height data in the version 4.2x Level 2 product is from 261 hPa to 0.001 hPa (Livesey et al., 2017), with the measurement errors of ±25 m, ±45 m, ±110 m, and ±160 m at 1 hPa, 0.1 hPa, 0.01 hPa, and 0.001 hPa. A comprehensive study of the measurement errors and fitting errors has been reported by Yamazaki and Matthias (2019) when using the Aura/MLS geopotential height data to obtain the amplitudes of Q5DOs. They have suggested that the mean values of the estimated 1-σ uncertainties in TPWs are about 50 m at high latitudes in the Northern Hemisphere. Following their technique, mean values of the estimated 1-σ uncertainties in the fitted amplitudes obtained by the new method are also about 50 m. The vertical structure of the estimated 1-σ uncertainty of the new method is the same as the distributions shown in Yamazaki and Matthias (Figure 1, 2019). In the present study, we focus on the difference between the original and new fitting methods. The fitted amplitudes are presented in the following analyses without dropping the values that are lower than the uncertainties. The analysis of this study focuses on the traveling Q5DOs with zonal wavenumbers of 1 and 2 based on the data at 60°N (averaged from 55-65°N).

3. Methodology

3.1 Simulations of the least-square fitting method

The least-square fitting method used in previous studies to derive the amplitude and phase of Q5DOs from satellite observations is based on equation (1) but without fitting the first term on the right-hand side (e.g., Huang et al., 2017; Qin et al., 2021). Generally, a 20-day sliding window with a step of one day is used to simultaneously extract the amplitudes of TPWs with zonal wavenumbers from 3 to -3 (westward to eastward). The daily amplitudes of the Q5DOs are obtained with the largest value in the wave periods between 4 and 7 days. The fitting result is marked at the end day of each 20-day window. To better understand the original least-square fitting method, the synthetic data are used to first~~ly~~ simulate the effect of a rapid and large change in SPWs when calculating the amplitudes of Q5DOs. As shown in Figures 1a and 1b, three components of waves with the zonal wavenumber of 1 are given in the synthetic data, which are an SPW with the amplitude of 100 m, eastward and westward propagating Q5DOs with amplitudes of 100 m and 60 m, respectively. The phases are respectively set as 0, $-\pi/4$, and $\pi/5$ for the SPW and the westward and eastward propagating Q5DOs. To simulate the effect of SPWs on TPWs, rapid large changes are given in the amplitudes of SPW on day 100 with magnitudes from 100 m to 500 m and on day 150 with magnitudes from 500 m to 100 m (see Figure 1a).

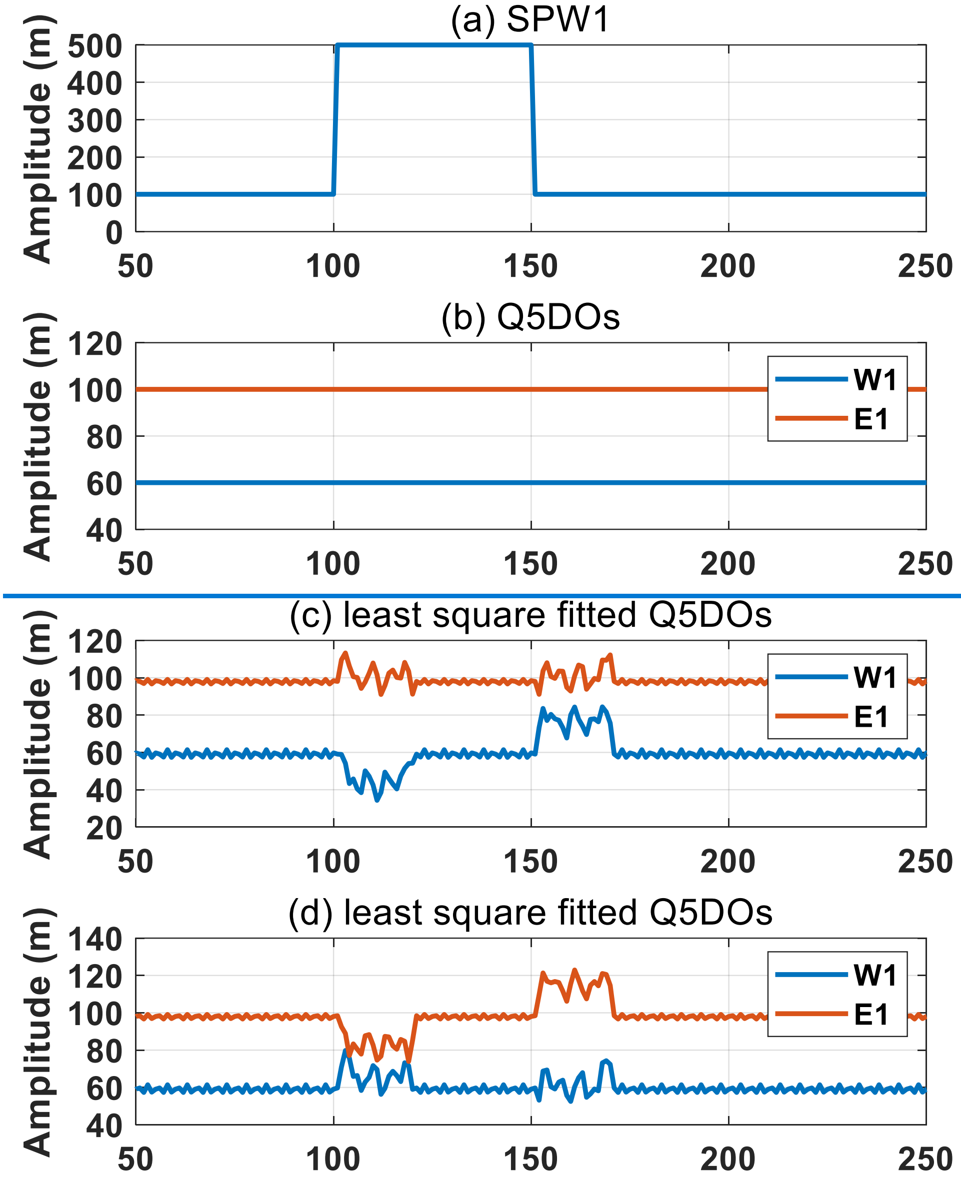
(a) SPW1
Amplitude (m)
500
400
300
200
100
0
50
100
150
200
250
(b) Q5DOs
Amplitude (m)
120
100
80
60
40
W1
E1
(c) least square fitted Q5DOs
Amplitude (m)
120
100
80
60
40
20
W1
E1
(d) least square fitted Q5DOs
Amplitude (m)
140
120
100
80
60
40
W1
E1

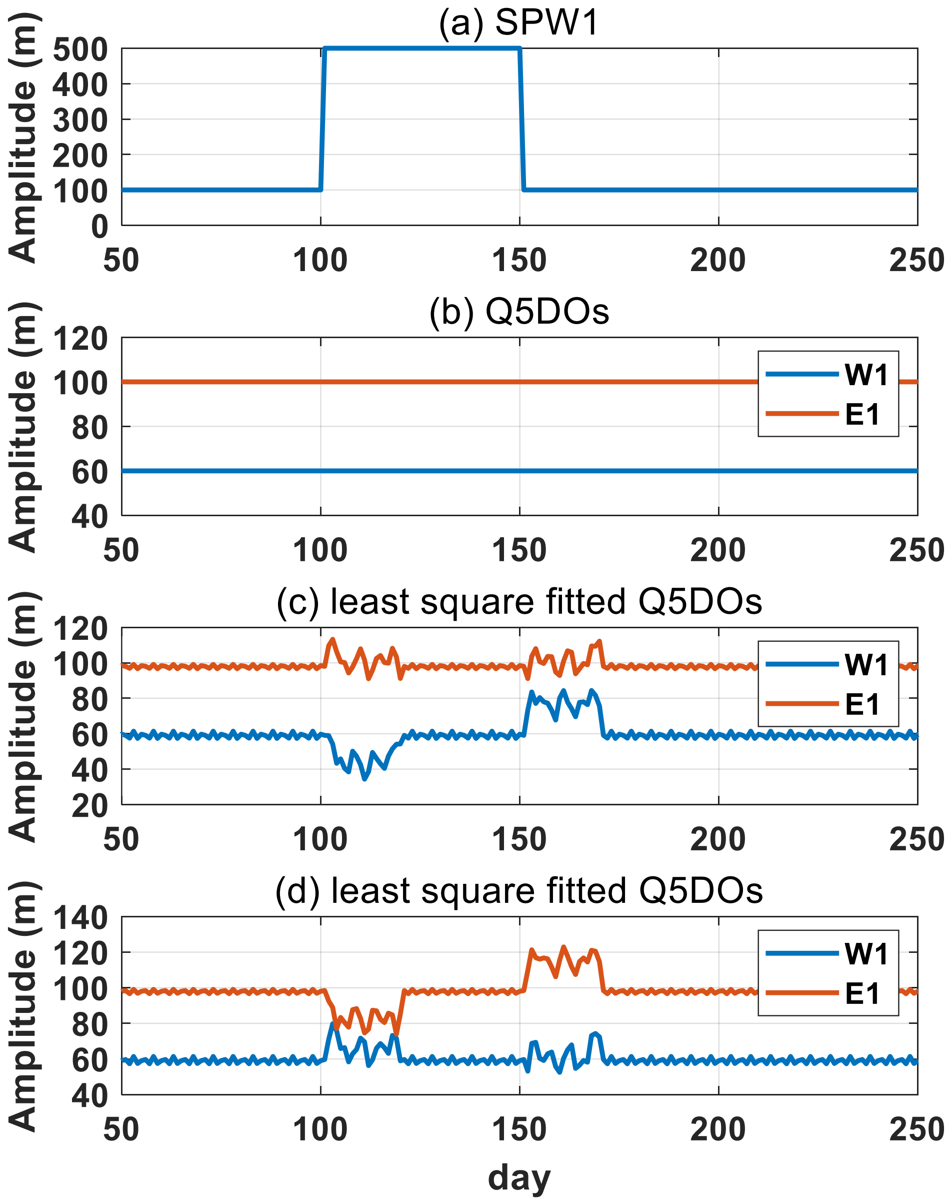

Figure 1. Simulations of the least-square fitting method based on synthetic data, which includes an SPW and westward and eastward Q5DOs with zonal wavenumber of 1. (a) Daily variations of the SPW amplitudes. The phase of the SPW is 0. (b) The real amplitudes of Q5DOs. Amplitudes are separately set as 100 m and 60 m for the eastward and westward Q5DOs. (c) Q5DOs obtained from the least-square fitting method. The phases are -π/4 and π/5 for the westward and eastward Q5DOs,

respectively. (d) Same as (c) but with phases of π/4 and -π/5 for the westward and eastward Q5DOs.

Figure 1c presents the amplitudes of the westward and eastward propagating Q5DOs fitted by the least--square fitting method. As shown in Figure 1c, abnormal fluctuations after day 100 and day 150 are captured, which correspond to the occurrence of rapid large changes in the amplitudes of SPW. However, Figure 1c suggests that the fitted Q5DOs are not largely influenced by the SPWs when rapid large changes are not given in the amplitudes of SPWs (before day 100 or from day 120 to 150). Additionally, Figure 1c indicates that abnormal fluctuations in Q5DOs induced by SPWs are not equivalent to two oppositely propagating directions. An enhancement and a decrease in the amplitudes of westward and eastward propagating Q5DOs can be simultaneously observed. Results shown in Figure 1d are the same as that in Figure 1c but are derived based on different phases of the westward and eastward Q5DOs in the synthetic data, where π/4, and -π/5 are given in the westward and eastward Q5DOs. Comparing the results between Figures 1c and 1d, it is interesting to note that the effect of a rapid large change in SPWs on the derived Q5DOs also depends on the phase relationships. Yamazaki and Matthias (2019) suggested that the effect of SPWs could be ignored when the activities of Q10DWs in the oppositely propagating direction were not simultaneously enhanced. However, according to our simulations, this criterion does is not suitable for the analysis of Q5DOs with different phases. Our simulation indicates that the influence of a quick and large change of SPW should not be ignored when extracting Q5DOs during SSWs from satellite observations based on the least least-square fitting method. Thus, in this study, we develop a new fitting method to derive the Q5DOs by suppressing the effect of a rapid and large change in SPWs.

3.2 New fitting method

Since the daily amplitude of SPW ($A_k(t)$) cannot be directly derived when Q5DOs exist, the primary goal of the new method is to eliminate the rapid and large changes in $A_k(t)$. The following steps are performed, where SPWs and Q5DOs are considered within the same wavenumbers.

Step 1. Estimate the daily variations of SPWs.

Based on the definition of SPW, the phase φ_k should be a fixed value in each window. Therefore, φ_k is first fitted based on $\mathrm{y}(x) = a_k \cos(kx - \varphi_k)$, where $\mathrm{y}(x)$ is the time-averaged geopotential height in each 20-day window. Using the fitted phase φ_k, the daily amplitudes of SPW can be roughly estimated by the least-square fitting based on equation (2), which equals equation (1).

$$\mathrm{Y}(x,t) = [A_k(t) + B_w \cos(\omega t - \varphi_w + \varphi_k) + B_e \cos(\omega t - \varphi_e - \varphi_k)] \cos(kx - \varphi_k)$$
$$+[B_e \sin(\omega t - \varphi_e - \varphi_k) - B_w \sin(\omega t - \varphi_w + \varphi_k)] \sin(kx - \varphi_k) \quad (2)$$

If we let $a_k(t) = A_k(t) + B_w \cos(\omega t - \varphi_w + \varphi_k) + B_e \cos(\omega t - \varphi_e - \varphi_k)$, and $b_k(t) = B_e \sin(\omega t - \varphi_e - \varphi_k) - B_w \sin(\omega t - \varphi_w + \varphi_k)$, equation (2) can be simply expressed as equation (3):

$$\mathrm{Y}(x,t) = a_k(t) \cos(kx - \varphi_k) + b_k(t) \sin(kx - \varphi_k) \quad (3)$$

However, the fitted amplitudes of SPWs, $a_k(t)$, are not the true amplitudes of SPWs ($A_k(t)$), which includes the aliasing from Q5DOs. According to the above two equations, rapid and large changes in SPW amplitudes can only have impacts on the values of $a_k(t)$. Because the true values of $A_k(t)$ cannot be directly fitted due to the aliasing of Q5DOs, our goal in Step 2 is to eliminate the rapid large changes in $a_k(t)$.

Step 2. Eliminate the large rapid changes in SPWs.

If we let $P_k(t) = B_w \cos(\omega t - \varphi_w + \varphi_k) + B_e \cos(\omega t - \varphi_e - \varphi_k) = P\cos(\omega t - \varphi)$, $a_k(t)$ in Equation (3) can be also expressed as,

$$a_k(t) = A_k(t) + P_k(t) = A_k(t) + P\cos(\omega t - \varphi) \tag{4}$$

The amplitude P and phase φ can be estimated by the ~~least~~ least-square fitting via equation (4). Taking the partial derivatives in time on both sides of equation (4), we obtain equation (5):

$$\frac{\partial}{\partial t} a_k(t) = \frac{\partial}{\partial t} A_k(t) + \frac{\partial}{\partial t} P_k(t) \tag{5}$$

where $\frac{\partial}{\partial t} A_k(t)$ are the daily variations in the amplitudes of SPW. The primary goal of Step 2 is to subtract large values of $\frac{\partial}{\partial t} A_k(t)$ from $a_k(t)$ to eliminate the large variations in $a_k(t)$. However, $\frac{\partial}{\partial t} A_k(t)$ cannot be obtained simply by $\frac{\partial}{\partial t} A_k(t) = \frac{\partial}{\partial t} a_k(t) - \frac{\partial}{\partial t} P_k(t)$, because $\frac{\partial}{\partial t} P_k(t)$ cannot be derived accurately when $\left|\frac{\partial}{\partial t} A_k(t)\right|$ are large ("| |" represents the absolute values). Nevertheless, the lower boundary of the values in $\left|\frac{\partial}{\partial t} a_k(t)\right|$ can be estimated when rapid large changes exist in SPWs ($\left|\frac{\partial}{\partial t} A_k(t)\right|$ are large). The maximum value in $\left|\frac{\partial}{\partial t} a_k(t)\right|$ will be at least larger than the maximum value in $\frac{\partial}{\partial t} P_k(t) = -\omega P\sin(\omega t - \varphi)$, which is ωP. Thus, the value of ωP can be used as a threshold to determine rapid large changes in SPWs.

Therefore, when $\left|\frac{\partial}{\partial t} a_k(t)\right|$ are larger than the threshold of ωP, we subtract the value of the corresponding $\frac{\partial}{\partial t} A_k(t)$ from all the following members of $a_k(t)$ to obtain a new series of $a_k^{new}(t)$. The $\frac{\partial}{\partial t} A_k(t)$ are estimated by $\frac{\partial}{\partial t} A_k^{estimated}(t) =$

$\frac{\partial}{\partial t} a_k(t) - \frac{\partial}{\partial t} P_k^{estimated}(t)$, where $P_k^{estimated}(t) = P_{pre}\cos\big(\omega(t+1) - \varphi_{pre}\big)$. Instead of the P and φ fitted in the present window, the P_{pre} and φ_{pre} fitted from the previous one are used because the fitted P_{pre} and φ_{pre} are not influenced by the effect of rapid large changes in SPWs in the present window. Here, we have a new series of $a_k^{new}(t)$ without rapid large changes in SPWs, as well as new fitted P and φ for the next window.

Step 3. Fit the real amplitudes of Q5DOs.

After obtained the $a_k^{new}(t)$ and $b_k(t)$ from Step 2, the reconstruction of the original data $Y'(x,t)$, which inhibits the rapid and large changes in SPWs, can be reconstructed based on equation (6):

$$Y'(x,t) = a_k^{new}(t)\cos(kx - \varphi_k) + b_k(t)\sin(kx - \varphi_k) \tag{6}$$

Then, the real amplitudes and phases of the Q5DOs (B_w, B_e, φ_w, and φ_e) can be fitted using the ~~least~~ least-square fitting method via $Y'(x,t) = B_w\cos(\omega t + kx - \varphi_w) + B_e\cos(\omega t - kx - \varphi_e) + C$, where C is a constant.

Note that, the effect of small changes in SPWs cannot be eliminated sometimes when $\left|\frac{\partial}{\partial t} a_k(t)\right|$ are smaller than ωP. These small changes in SPWs do not have significant effects on the fitted Q5DOs and their elimination depends on the phase relationships between westward and eastward Q5DOs. Nevertheless, the Monte Carlo simulations based on random phases of Q5DOs reveal~~s~~ that the fake fluctuations in Q5DO amplitudes due to this effect will not exceed the value of $0.1\omega P$.

4. Results and Discussions

4.1 Simulations

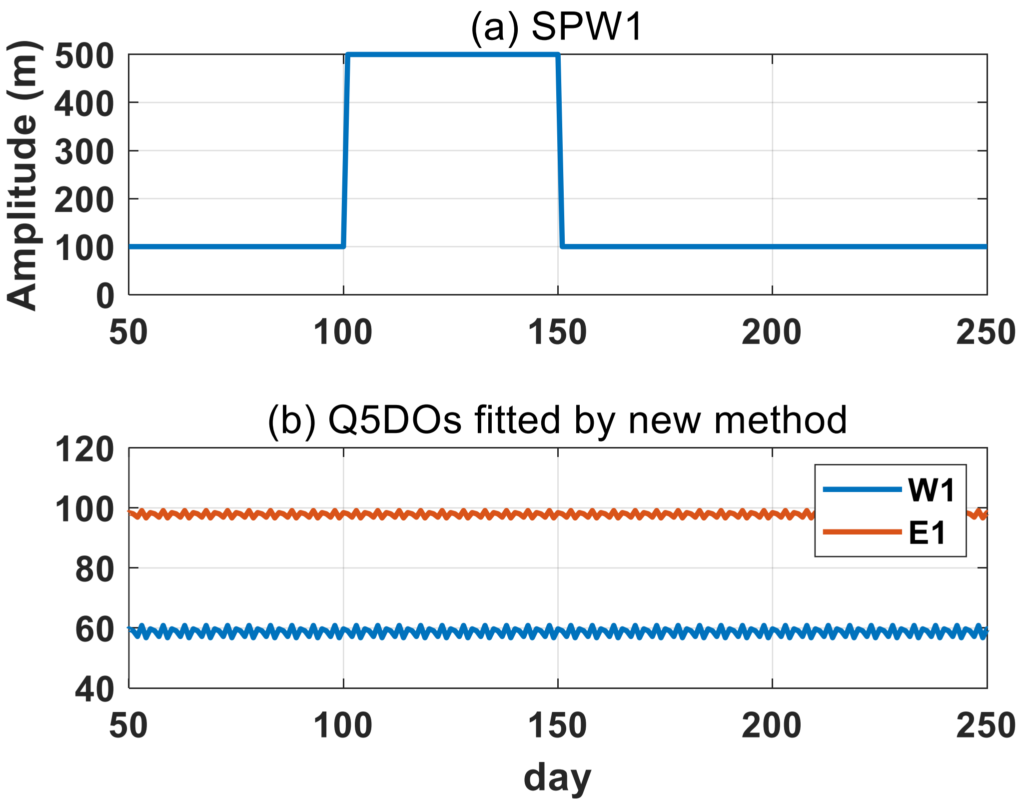

Figure 2. Simulations of the new fitting method based on synthetic data, which includes an SPW and westward and eastward Q5DOs with zonal wavenumber of 1. (a) Daily variations of the SPW amplitudes. The phase of the SPW is 0. (b) Q5DOs obtained from the new fitting method. The amplitudes are 60 m and 100 m, the phases are -π/4 and π/5 for the westward and eastward Q5DOs, respectively.

Based on the new fitting method, we present the fitting result in Figure 2. As shown in Figure 2b, the fitted amplitudes of the Q5DOs are generally consistent with the amplitudes given in the original synthetic data. The apparent fluctuations in Q5DOs induced by SPWs have been removed. Note that~~,~~ based on the new fitting method, the

~~fitting~~ fitted amplitudes ~~of the new method~~ are~~–~~ not dependent on the phases of Q5DOs. The new fitting method will provide the same results as those shown in Figure 2b when Q5DOs have different phases (~~the same as those shown in Figure 2b~~ not shown)~~when Q5DOs have different phases (not shown)~~. Thus, the fitted amplitudes from the new method do not rely on the phase relationships of those waves. Figure 2 demonstrates that the new method is effective to suppress the effect of large rapid change in SPWs, while ~~additional~~ a further experiment ~~where~~ that synthetic data containing the enhancement of both SPWs and Q5DOs ~~is~~ is needed to demonstrate that the new method can properly capture the changes of Q5DOs during SSWs. Besides, we also add signals of SPWs and Q5DOs with wavenumber 2 in the synthetic data to ~~establish a simulation that can model~~ approach the real situation in satellite observations. Figure 3 shows the results of ~~an additional~~the further experiment. The synthetic data used in Figure 3 consist of six components: SPWs with wavenumber 1 and 2 (SPW1 and SPW2), westward propagating Q5DOs with wavenumber 1 and 2 (W1 and W2), and eastward propagating Q5DOs with wavenumber 1 and 2 (E1 and E2). The daily variation of the amplitudes for SPWs and Q5DOs are separately shown in Figures 3a and 3b. The phase of SPW1, SPW2, and W1, E1, W2, and E2 Q5DOs are respectively set as 0, $\pi/6$, $-\pi/4$, $\pi/5$, $-\pi/4$, and $\pi/3$. Figures 3c and 3d present the fitting results for the ~~least~~ least-square fitting method and the new fitting method. As shown in Figure 3d, the result manifests that the variations of Q5DOs can be captured based on the new method and the effect of large rapid change in SPWs can be limited.

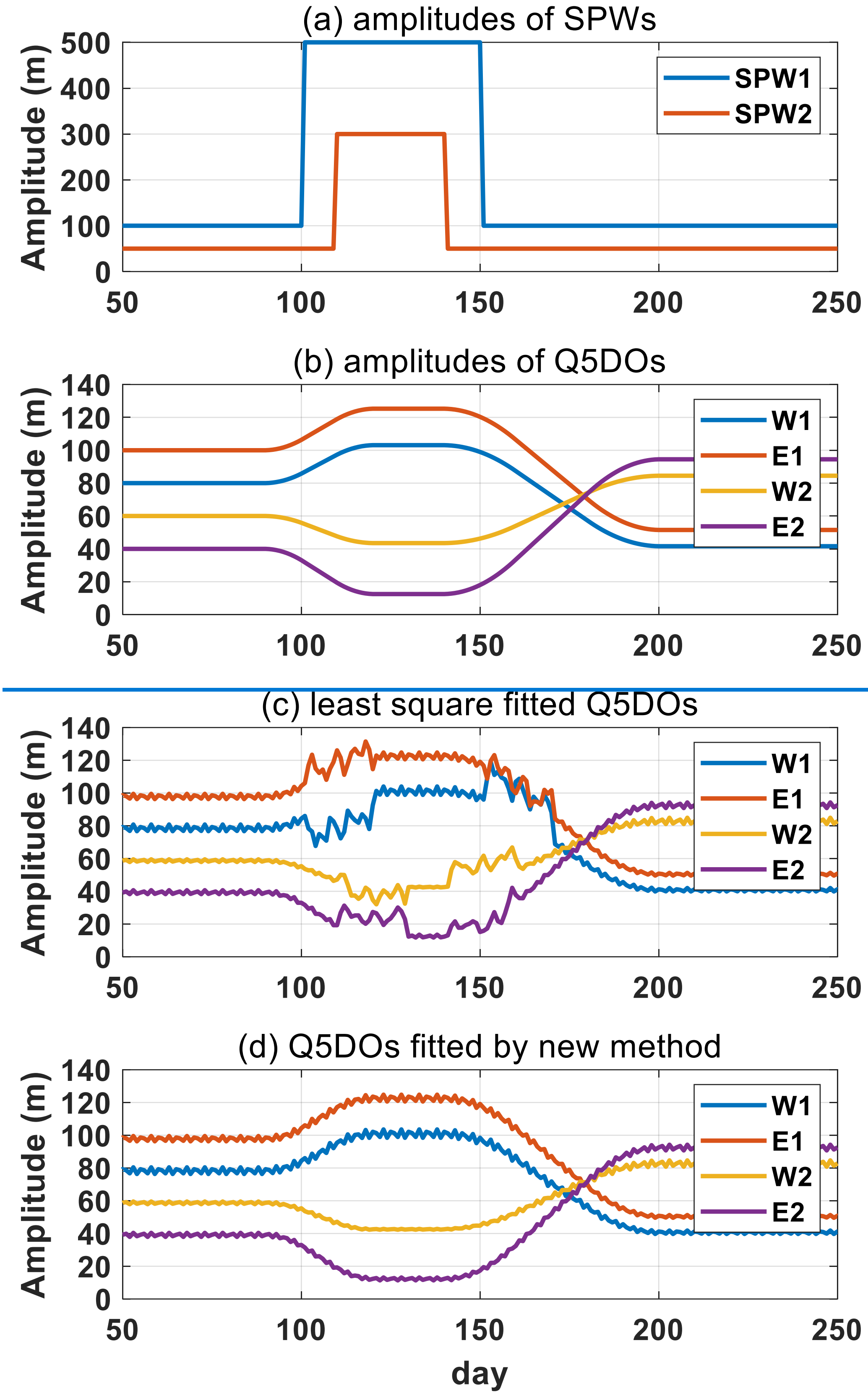
(a) amplitudes of SPWs
Amplitude (m)
500
400
300
200
100
0
50
100
150
200
250
SPW1
SPW2
(b) amplitudes of Q5DOs
Amplitude (m)
140
120
100
80
60
40
20
0
50
100
150
200
250
W1
E1
W2
E2
(c) least square fitted Q5DOs
Amplitude (m)
140
120
100
80
60
40
20
0
50
100
150
200
250
W1
E1
W2
E2
(d) Q5DOs fitted by new method
Amplitude (m)
140
120
100
80
60
40
20
0
50
100
150
200
250
day
W1
E1
W2
E2

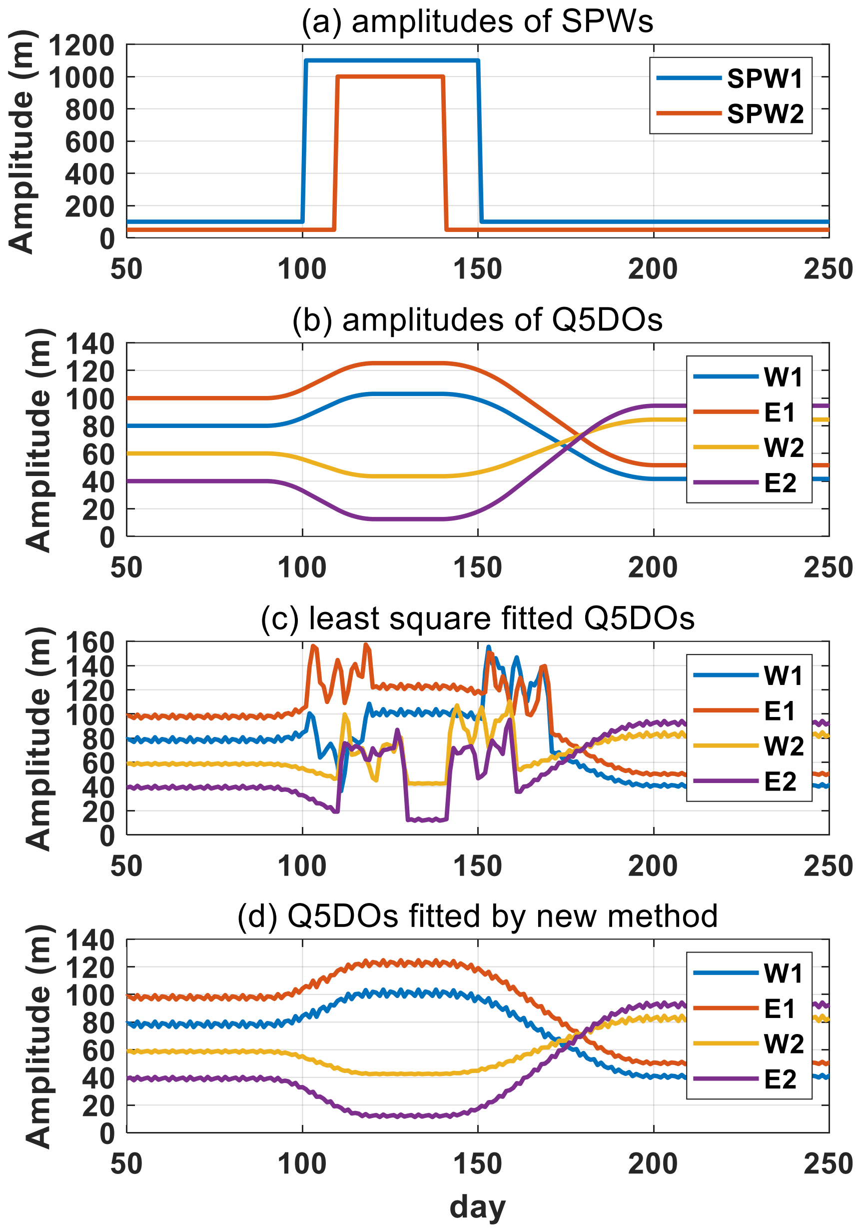

Figure 3. Simulations of the new fitting method based on synthetic data, which include (a) SPW1 and SPW2 and (b) westward and eastward Q5DOs with zonal wavenumber of 1 and 2. The phase of SPW1, SPW2, and W1, E1, W2, and E2 Q5DOs are respectively set as 0, π/6, -π/4, π/5, -π/4, and π/3. (c) Daily amplitudes of the fitted Q5DOs obtained from the original least-square fitting method. (d) Daily amplitudes of the fitted Q5DOs obtained from the new fitting method.

Note that some sawtooth-shaped points can be seen in the fitting results in Figures 1, 2, and 3. The sawtooth-shaped points are caused by removing the linear declination on the time series. This process needs to be done in both original and new methods to eliminate the effect of seasonal trends in the observational data on the fitting of Q5DOs. The sawtooth-shaped points can be eliminated in the simulation by not removing the seasonal trends, but we keep them in both original and new methods in the simulations in order to be consistent with the processes in dealing with the observational data.

4.2 Observations

The SPWs and TPWs can be both captured in the mesosphere region and their origins have been reported in some previous studies. The mesospheric SPWs are usually believed to be related to the upward wave signals from the troposphere and the lower stratosphere which rely on the structure of the polar vortex (e.g., Harvey et al., 2018). In addition, wave-wave interactions, gravity wave forcing, and auroral heating can also generate mesospheric SPWs (e.g., Lu et al., 2018; Xu et al., 2013; Smith, 2003). The mesospheric TPWs are generally considered as the result of atmospheric instabilities and many recent studies have noticed the relationship between extremely strong TPWs and SSW events (Liu et al., 2004; Ma et al., 2020; Yamazaki et al., 2021). The mesospheric TPWs during SSWs can be also secondarily generated in situ by wave-wave interactions (e.g., Xiong et al., 2018; Wang et al., 2021). Nevertheless, the trigger mechanisms of mesospheric TPWs are still not fully understood due to a lack of long-term and high-resolution observational data in this region. Thus, satellite observations are widely used to reveal the feature of mesospheric TPWs. However, as indicated by our simulations, the previous studies have ignored the effect of rapid and large changed SPWs when calculating the variations of TPWs during SSWs. Using the geopotential height data provided by the Aura/MLS measurement, we extract the variations of the traveling Q5DOs at 60°N during Arctic SSWs. The effectiveness of the new fitting method is discussed by comparing the results between the original ~~least-~~ least-square fitting method and the new method. The daily amplitudes of the Q5DOs are obtained with the largest value in the wave periods between 4 and 7 days. The fitting result is marked at the end day of each 20-day window. The traveling Q5DOs with wavenumber 3 and the amplitudes below 10 hPa are not shown due to their weak amplitudes. In the present study, the pressure regions from 10 hPa to 1 hPa, from 1 hPa to 0.01 hPa, and from 0.01 hPa to 0.001 hPa are respectively discussed as the stratosphere, mesosphere, and lower thermosphere.

Since the observation of the Aura satellite is available after August 2004, the variations of traveling Q5DOs are investigated during eight mid-winter major SSWs from 2005 to 2021 in the present study. Table 1 presents the eight mid-winter major SSWs with their onset dates. The date with the maximum positive temperature gradient between 90°N and 60°N at 10 hPa is defined as the SSW onset date, which is obtained around the date of the first wind reversal during each major event (e.g., Andrews et al., 1987). Note that the onset date used in the present study is only to roughly determine the commencement of SSWs and our discussions are not sensitive to the non-uniformed definitions of SSW onsets (e.g., Butler et al., 2015). In the present study, the SSW in the winter of 2009/2010 is classified as a minor one, because the wind reversal occurred too late (18 days after the onset date) without any positive temperature gradient between 90°N and 60°N at 10 hPa. To be distinguished from the SSW in February 2018, the SSW with the onset date of December 28, 2018, is discussed as the "2019 SSW" in this study. The SSWs before 2013 have been widely studied in previous studies (e.g., Choi et al., 2019; Charlton and Polvani, 2007; Butler et al., 2017; Liu et al., 2019; Rao et al., 2019), details of the three major SSWs from 2018 to 2021 can be referred to many recent reports (e.g., Rao et al., 2018, 2020, 2021; Wang et al., 2019; Davis et al., 2022; Okui et al., 2021; Wright et al., 2021).

Table 1. Mid-winter major SSWs from 2005 to 2021.

SSW	Onset Date	First Wind Reversal Date
2006	January 22, 2006	January 21, 2006
2007	February 24, 2007	February 24, 2007
2008	February 23, 2008	February 22, 2008
2009	January 23, 2009	January 24, 2009
2013	January 6, 2013	January 6, 2013
2018	February 11, 2018	February 12, 2018
2019	December 28, 2018	January 2, 2019
2021	January 4, 2021	January 5, 2021

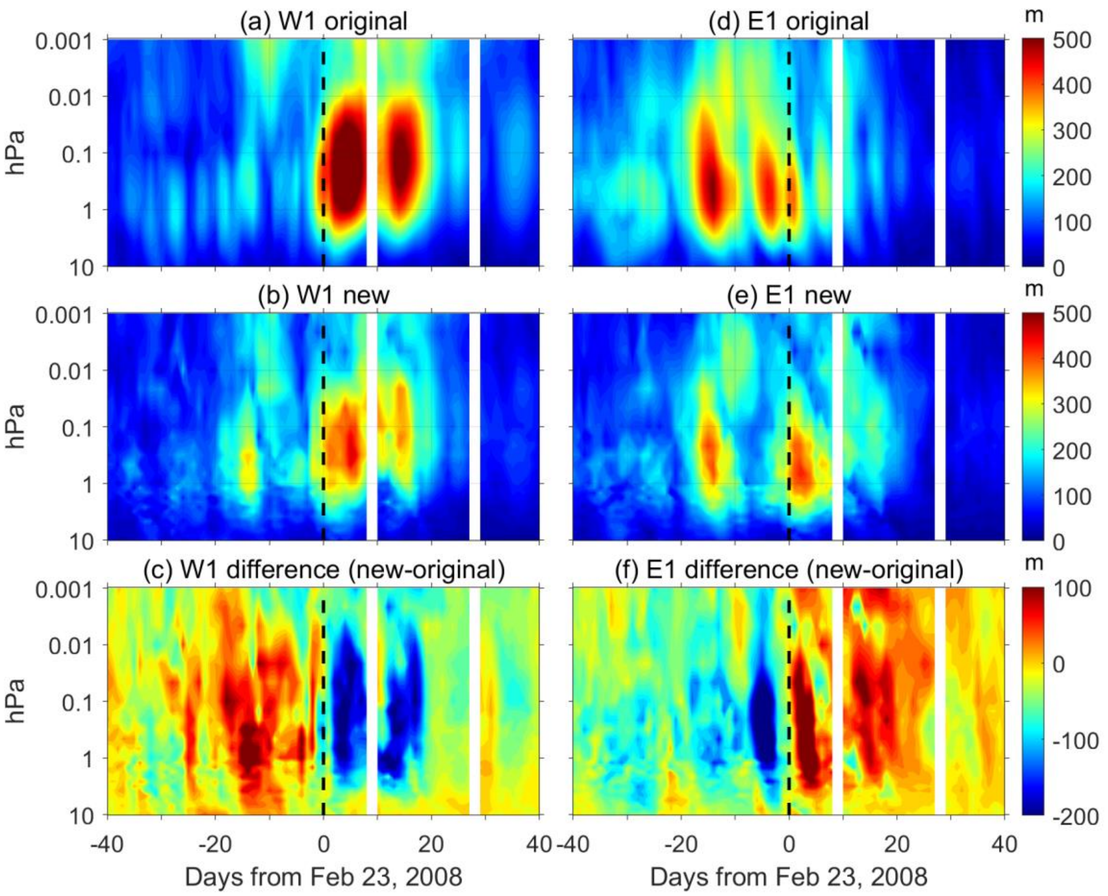

Figure 4. The amplitudes of W1 (left column) and E1 (right column) Q5DOs during the 2008 SSW obtained by the original least-square fitting method (top row) and the new fitting method (middle row). The differences between the new and original methods are shown in the bottom row (c and f). Contour steps are 10 m.

Comparisons of fitted amplitudes of traveling Q5DOs are first shown in Figures 4 and 5, respectively for wavenumber 1 during the 2008 SSW and wavenumber 2 during the 2013 SSW. Results for each case are given in 81 days, which is from 40 days before to 40 days after the SSW onset date (day 0). Figure 4 presents the amplitudes of W1 and E1 Q5DOs obtained from both original (top) and new (middle) methods during the 2008 SSW. The differences are calculated by subtracting the fitting result of the original method from the new method, which are given at the bottom of Figure 4. Amplitudes are not fitted in the white area where the available data are less than 60% in each window. As shown in Figure 4a, the W1 Q5DOs fitted by the original least~~-~~-square fitting method reveal a significant response to the onset of 2008 SSW. The amplitudes of the W1 Q5DOs in the mesosphere are larger than 500 m from day 0 to day 20 with a maximum amplitude of 628 m on day 5. Figure 4b suggests that the amplitudes obtained from the new method are lower than 500 m during the 2008 SSW. The maximum amplitude obtained from the new method is 466 m on day 5, which is about 75% of the amplitude obtained from the original ~~least~~ least-square fitting method. The negative differences shown in Figure 4c are generally larger than 200 m from day 0 to day 20 in the mesosphere, which indicates that the amplitudes of W1 Q5DOs after the onset of 2008 SSW ~~are~~ might be ~~largely~~ overestimated by the original ~~least~~ least-square fitting method. Nevertheless, positive differences larger than 100 m are also captured before the SSW onset (day -15) around 1 hPa as shown in Figure 4c, which reveals that the amplitudes of W1 Q5DOs obtained from the original method can be also underestimated during the 2008 SSW. For the amplitudes of E1 Q5DOs during the 2008 SSW, the original ~~least~~ least-square fitting method ~~has~~ may have an overestimation before the onset date and an underestimation after the onset date. As shown in Figure 4f, the positive and negative differences both have maximum amplitudes over 200 m in the mesosphere around the onset date.

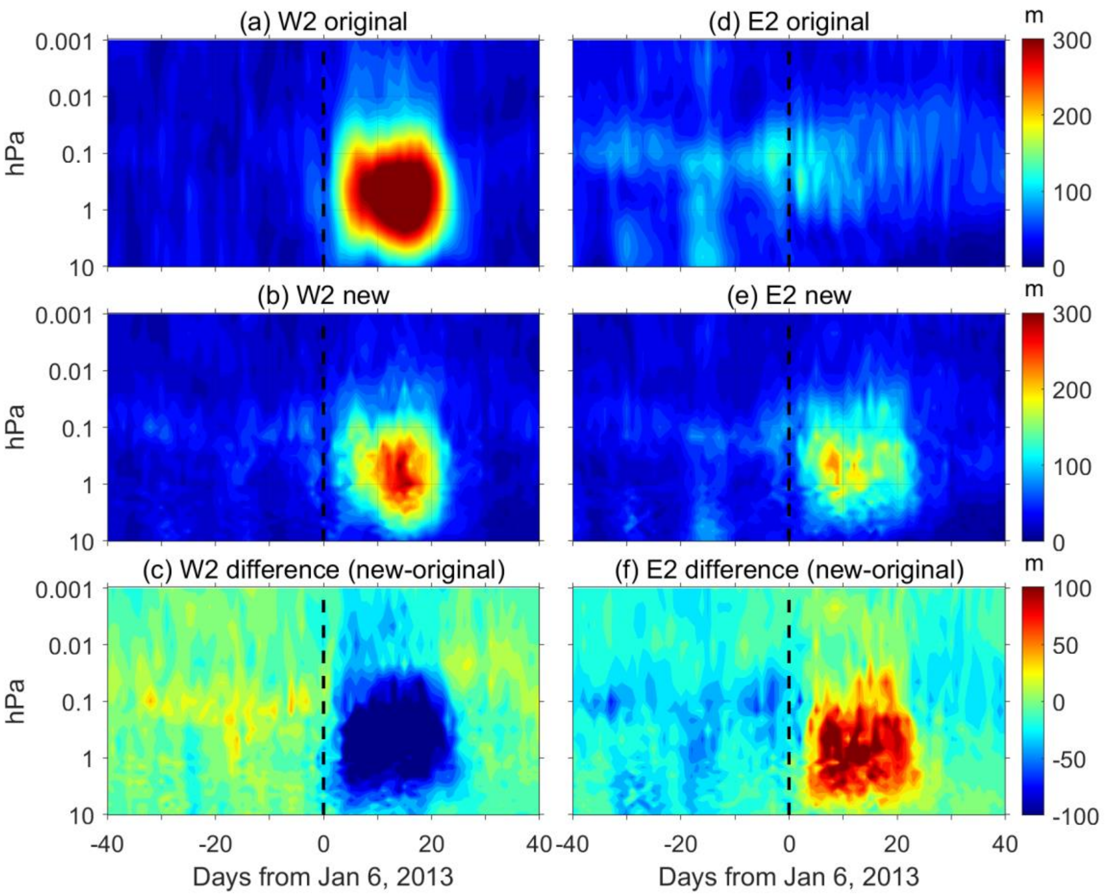

Figure 5. Same as Figure 4 but for W2 and E2 Q5DOs during the 2013 SSW.

Figure 5 presents the same results as Figure 4 but for the amplitudes of W2 and E2 Q5DOs during the 2013 SSW. As shown in Figure 5, strong enhancements of W2 Q5DOs and weak amplitudes of E2 Q5DOs after the 2013 SSW are captured by the original ~~least~~ least-square fitting method. However, results from the new method after the onset of 2013 SSW suggest that based on the original least-square fitting method, the amplitudes of W2 Q5DOs ~~are~~ might be overestimated and the amplitudes of E2 Q5DOs ~~are~~ may be underestimated. The maximum positive and negative differences are both over 100 m. In order to understand the common differences between the two methods, we calculate the differences during ~~all~~ the eight SSWs and present ~~a composite~~the results in Figures 6, 7, 8, and 9 for the W1, W2, E1, and E2 components, respectively.

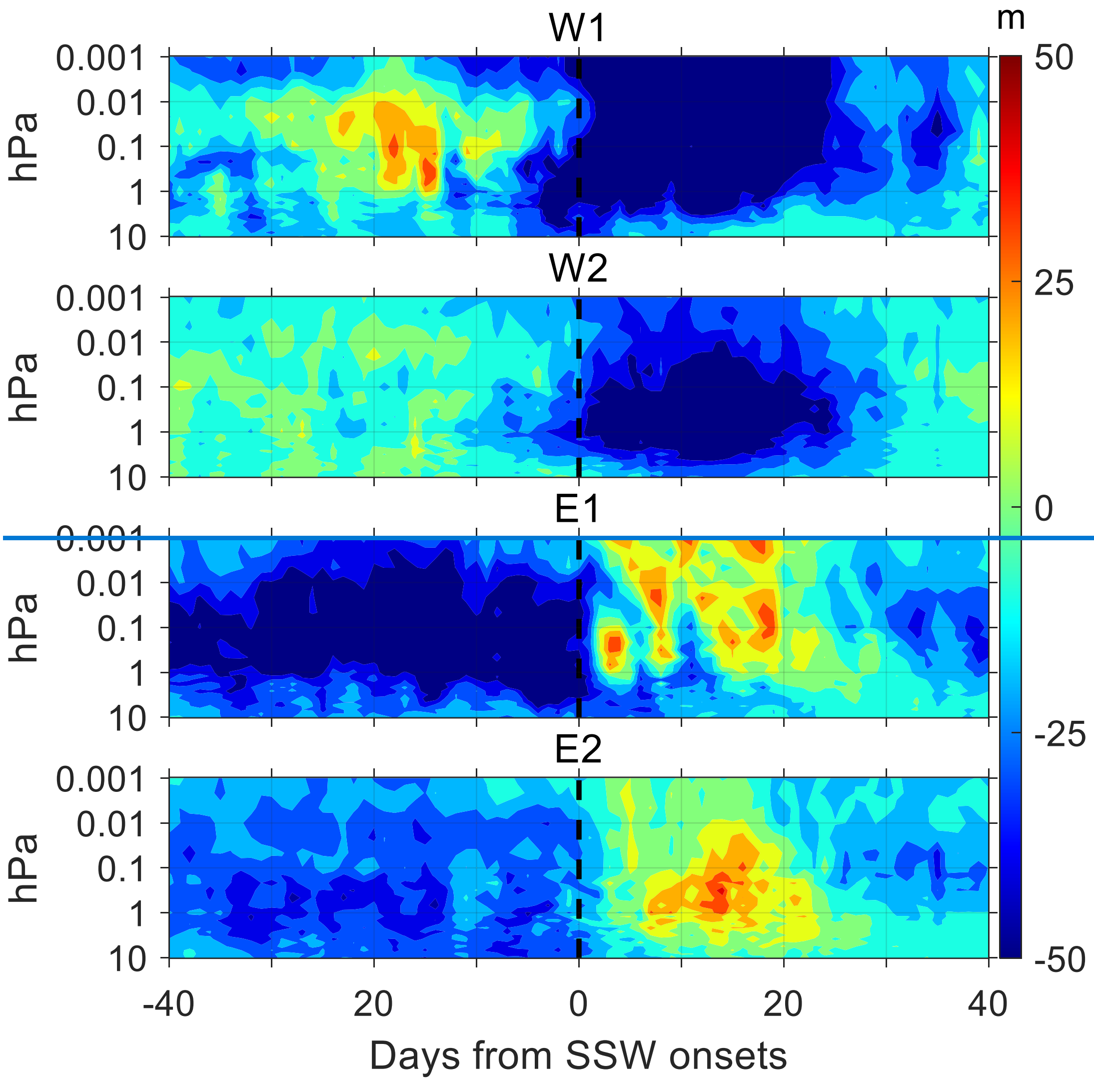

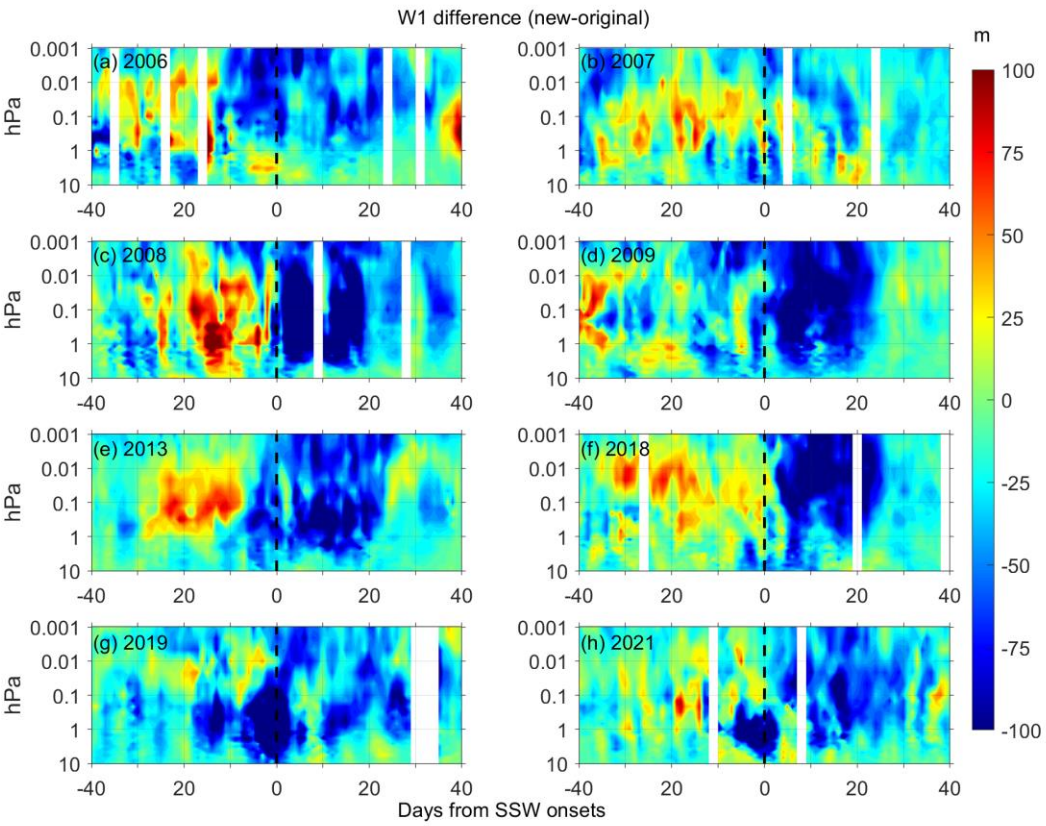

Figure 6. The differences in the fitted W1 Q5DO amplitudes between the new and original methods during 8 major SSWs since 2006 (from a to h). Contour steps are 5 m.~~The differences between the new and original methods for the W1, W2, E1, and E2 Q5DOs (from top to bottom). Contour steps are 10 m.~~

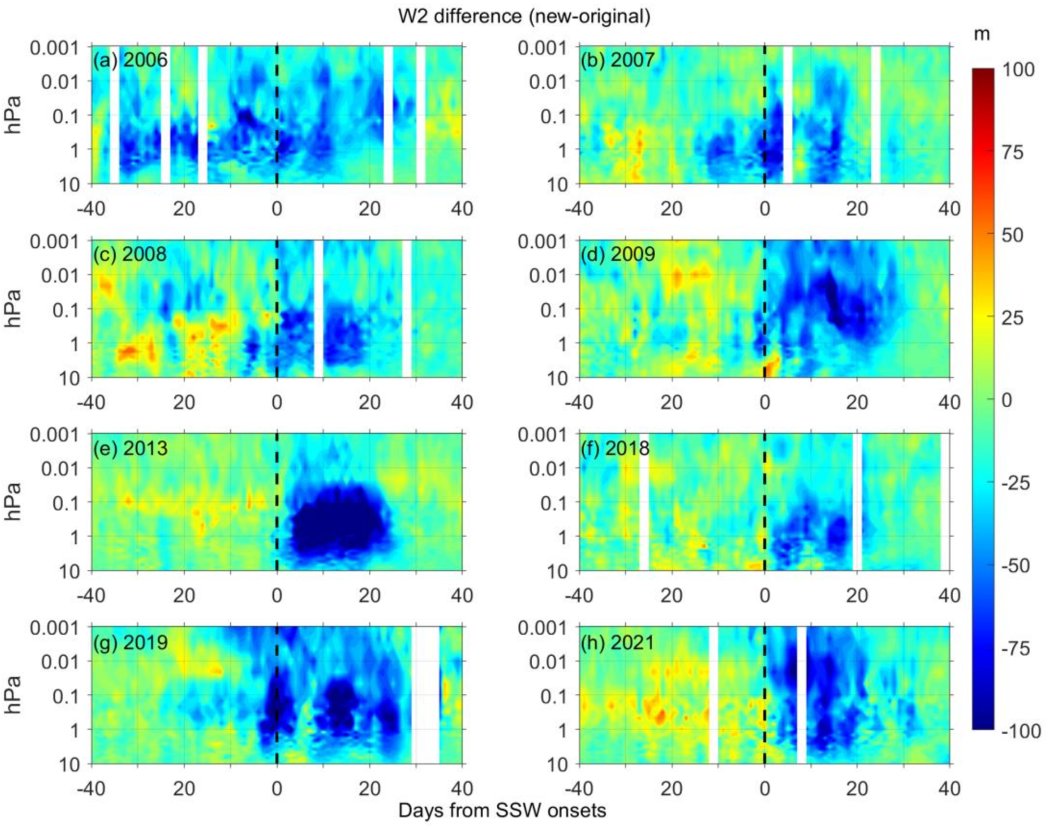

Figure 7. Same as Figure 6 but for the W2 component.

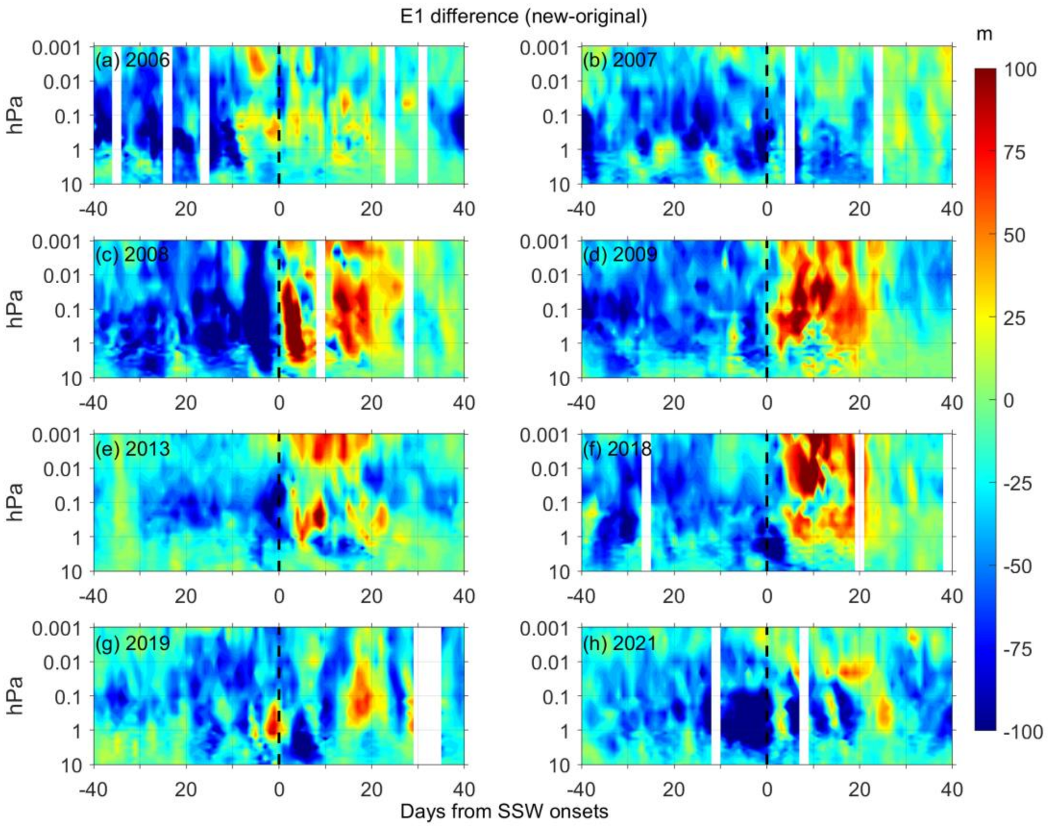

Figure 8. Same as Figure 6 but for the E1 component.

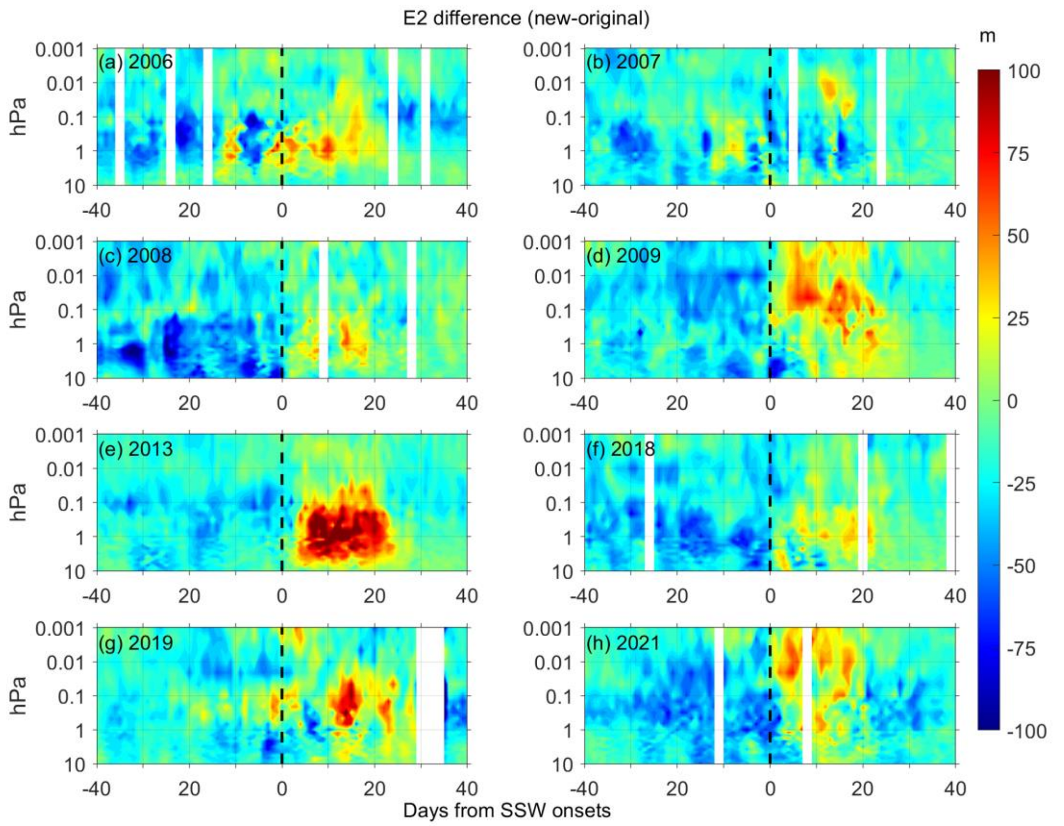

Figure 9. Same as Figure 6 but for the E2 component.

As shown in Figures 6 and 7, the difference in the fitted westward propagating Q5DO amplitudes between the new and original methods westward propagating Q5DOs are usually negative after the SSW onsets, which suggests that the amplitudes of the westward propagating Q5DOs might be overestimated by the original least--square fitting method after the SSW onsets-.after the SSW onsets, However, the difference in the fitted eastward propagating Q5DO amplitudes between the new and original methods (as shown in Figures 8 and 9) are usually positive after the SSW onsets, which indicates that while the eastward propagating Q5DOs the amplitudes of the eastward propagating Q5DOs might be underestimated by the original least-square fitting method after the SSW onsetsare mostly underestimated after the SSW onsets.

Additionally, ~~T~~the E1 Q5DOs before the SSW onsets ~~are~~ might be also overestimated by the original least~~-~~-square fitting method as seen in Figure ~~6c~~8. The enhancements of traveling Q5DOs during SSWs reported in previous studies are usually westward propagating after the SSW onsets and eastward propagating before the SSW onsets (e.g., Gong et al., 2018; Yu et al., 2022). Thus, our analyses indicate that the previously-reported Q5DOs obtained by satellite measurements during SSWs might be contaminated by SPWs. The amplitudes of the enhancement of Q5DOs during SSWs might be overestimated. Additionally, ~~Figure 6 reveals that~~ the westward propagating Q5DOs before the SSW onsets and the eastward propagating Q5DOs after the SSW onsets ~~are~~ might be underestimated by the original least~~-~~-square fitting method. Therefore, in future studies of the activities of Q5DOs during SSWs based on satellite observations and reanalysis data, the variations of different wave components in Q5DOs have to be carefully derived by eliminating the effects of SPWs.

Generally, the TPWs, including the Q5DOs, dominate in the mesosphere and lower thermosphere, which are enhanced seasonally during winter and spring times and largely control the neutral winds and temperatures in the middle atmosphere (e.g., Gong et al., 2018, 2019; Pancheva et al., 2018; Yamazaki et al., 2020, 2021). The vertical and latitudinal propagation of the TPWs can also transport energies and lead to couplings on a global scale (e.g., Koushik et al., 2020; Ma et al., 2022). Thus, extracting the real amplitudes of the traveling waves is also important to reveal the characteristics in the mesosphere and the vertical couplings in the middle atmosphere. Some extremely strong TPWs are found to be related to the occurrence of SSWs, but their trigger mechanisms have not been fully understood (e.g., Ma et al., 2020; Yamazaki et al., 2021). However, the rapid and large change of the SPWs during SSWs can lead to contaminations when deriving the real amplitudes of TPWs based on satellite observations or reanalysis data. The new method proposed in the present study can capture a more accurate variation in the amplitudes of TPWs than the old one. The new method is based on the examinations during SSWs due to the assumption that a rapid and large change in SPWs is usually observed during SSWs. Nevertheless, the new method can also be used to extract the amplitudes of TPWs in the mesosphere during other seasons and cases, such as the spring final warmings and other disturbances in stratospheric vortices. Based on the new method, the common feature of the TPWs revealed by satellite observations in the mesosphere and lower thermosphere can be reevaluated, and the trigger mechanism of the mesospheric TPWs during SSWs can be further understood.

5. Summary and conclusions

In the present study, a new fitting method is developed to derive the variations of traveling quasi-5-day waves (Q5DOs) by inhibiting the effect of rapid and large changes in the amplitudes of stationary planetary waves (SPWs). The effectiveness of the new method is demonstrated by both synthetic and observational data. According to the simulations, the new method can capture the variations of the amplitudes of traveling Q5DOs when large and rapid changes in SPWs are given. Based on the geopotential height data measured by MLS onboard the Aura satellite, we compare the difference of the traveling Q5DOs amplitudes between the original least-square fitting method and the new fitting method in the middle atmosphere during eight Arctic major SSWs from 2005 to 2021. Our results indicate that the enhancements of traveling Q5DOs during SSWs reported in previous studies might be overestimated due to ignoring the effect of large rapid changes in SPWs. Besides, the amplitudes of westward propagating Q5DOs before the SSW onsets and the amplitudes of eastward propagating Q5DOs after the SSW onsets might be underestimated. Note that since the amplitudes of SPWs cannot be derived accurately due to the aliasing of Q5DOs, the contribution of the SPWs and Q5DOs during SSWs cannot be quantified in the present method. Our goal is to attenuate the effect of SPWs on the derivation of Q5DOs during SSWs. Future works are needed to examine the effectiveness of the new method by using traveling planetary oscillations with other periods, such as the quasi-10-day and quasi-16-day waves.

Data availability. The Aura/MLS geopotential height data can be downloaded through the Goddard Earth Sciences Data and Information Services Center via (https://acdisc.gesdisc.eosdis.nasa.gov/data/Aura_MLS_Level2/ML2GPH.004/).

Author contributions. ZM and YG proposed the scientific ideas. QX and ZM contributed to data processing and simulation programming. ZM, YG, and SZ completed the analysis and manuscript. CH and KH discussed the results in the manuscript.

Competing interests. The authors declare that they have no conflict of interest.

Acknowledgments. We acknowledge the Goddard Earth Sciences Data and Information Services Center for providing the Aura/MLS geopotential height data.

Financial support. This study is supported by the National Natural Science Foundation of China (through grants 42104145 and 41574142), the Fundamental Research Funds for the Central Universities 2042021kf0021, and the China Postdoctoral Science Foundation (through grants 2021M692465 and 2020TQ0230).

References

Andrews, D. G., Holton, J. R., and Leovy, C. B.: Middle Atmosphere Dynamics, 1st ed., Academic Press, San Diego, Calif, 1987.

Baldwin, M. P., Ayarzagüena, B., Birner, T., Butchart, N., Butler, A. H., and Charlton-Perez, A. J.: Sudden stratospheric warmings. Reviews of Geophysics, 58, e2020RG000708. https://doi.org/10.1029/2020RG000708, ~~2020~~2021.

Butler, A. H., Seidel, D. J., Hardiman, S. C., Butchart, N., Birner, T., and Match, A.: Defining Sudden Stratospheric Warmings, Bulletin of the American

Meteorological Society, 96(11), 1913-1928, https://doi.org/10.1175/BAMS-D-13-00173.1, 2015.

Butler, A. H., Sjoberg, J. P., Seidel, D. J., and Rosenlof, K. H.: A sudden stratospheric warming compendium. Earth System Science Data, 9, 63–76. https://doi.org/10.5194/essd-9-63-2017, 2017.

Charlton, A. J., and Polvani, L. M.: A new look at stratospheric sudden warmings. Part I: Climatology and modeling benchmarks. J. Climate, 20(3), 449–469. https://doi.org/10.1175/JCLI3996.1, 2007.

Choi, H., Kim, B. M., and Choi, W.: Type classification of sudden stratospheric warming based on pre- and postwarming periods. Journal of Climate, 32(8), 2349–2367. https://doi.org/10.1175/JCLI-D-18-0223.1, 2019

Davis, N.A., Richter, J.H., Glanville, A.A., Edwards, J., and LaJoie, E.: Limited surface impacts of the January 2021 sudden stratospheric warming. Nature Communications, 13, 1136. https://doi.org/10.1038/s41467-022-28836-1, 2022.

Domeisen, D. I. V., Butler, A. H., Charlton-Perez, A. J., Ayarzagüena, B., Baldwin, M. P., Dunn-Sigouin, E., Furtado, J. C., Garfinkel, C. I., Hitchcock, P., Karpechko, A. Yu., Kim, H., Knight, J., Lang, A. L., Lim, E., Marshall, A., Roff, G., Schwartz, C., Simpson, I. R., Son, S., Taguchi, M.: The role of the stratosphere in subseasonal to seasonal prediction: 2. Predictability arising from stratosphere-troposphere coupling. Journal of Geophysical Research: Atmospheres, 125, e2019JD030923. https://doi.org/10.1029/2019JD030923, 2020.

Gong, Y., Li, C., Ma, Z., Zhang, S., Zhou, Q., Huang, C., Huang, K., Li, G., Ning, B.: Study of the quasi-5-day wave in the MLT region by a meteor radar chain. Journal of Geophysical Research: Atmospheres, 123, 9474–9487. https://doi.org/10.1029/2018JD029355, 2018.

Gong, Y., Wang, H., Ma, Z., Zhang, S., Zhou, Q., Huang, C., and Huang, K.: A statistical analysis of the propagating quasi 16-day waves at high latitudes and their response to sudden stratospheric warmings from 2005 to 2018. Journal of Geophysical Research: Atmospheres, 124, 12,617-12,630. https://doi.org/10.1029/2019JD031482, 2019.

Harada, Y., and Hirooka, T.: Extraordinary features of the planetary wave propagation during the boreal winter 2013/2014 and the zonal wave number two predominance. Journal of Geophysical Research: Atmospheres, 122(21), 11374–11387. https://doi.org/10.1002/2017JD027053, 2017.

Harvey, V. L., Randall, C. E., Goncharenko, L., Becker, E., and France, J.: On the upward extension of the polar vortices into the mesosphere. Journal of Geophysical Research: Atmospheres, 123(17), 9171–9191. https://doi.org/10.1029/2018JD028815, 2018.

Huang, Y. Y., Zhang, S., Li, C. Y., Li, H. J., Huang, K., and Huang, C.: Annual and inter-annual variations in global 6.5DWs from 20–110 km during 2002–2016 observed by TIMED/SABER. Journal of Geophysical Research: Space Physics, 122, 8985–9002. https://doi.org/10.1002/2017JA023886, 2017.

King, A. D., Butler, A. H., Jucker, M., Earl, N. O., and Rudeva, I.: Observed relationships between sudden stratospheric warmings and European climate extremes. Journal of Geophysical Research: Atmospheres, 124(24), 13943–13961. https://doi.org/10.1029/2019JD030480, 2019.

Koushik, N., Kumar, K. K., Ramkumar, G., Subrehmanyam, K. V., Kishore Kumar, G., Hocking, W. K., He, M., Latteck, R.: Planetary waves in the mesosphere lower thermosphere during stratospheric sudden warming: Observations using a network of meteor radars from high to equatorial latitudes. Climate Dynamics, 54(9–10), 4059–4074. https://doi.org/10.1007/s00382-020-05214-5, 2020.

Kozubek, M., Krizan, P., and Lastovicka, J.: Northern Hemisphere stratospheric winds in higher midlatitudes: longitudinal distribution and long-term trends. Atmos. Chem. Phys., 15(4), 2203–2213. https://doi.org/10.5194/acp-15-2203-2015, 2015.

Lawrence, Z. D., and Manney, G. L.: Characterizing stratospheric polar vortex variability with computer vision techniques. Journal of Geophysical Research: Atmospheres, 123(3), 1510–1535., 2018.

Lin, J. T., Lin, C. H., Rajesh, P. K., Yue, J., Lin, C. Y., and Matsuo, T.: Local-time and vertical characteristics of quasi-6-day oscillation in the ionosphere during the 2019 Antarctic sudden stratospheric warming. Geophysical Research Letters, 47. https://doi.org/10.1029/2020GL090345, 2020.

Livesey, N. J., Read, W. G., Wagner, P. A., Froidevaux, L., Lambert, A., Manney, G. L., Millan Valle, L. F., Pumphrey, H. C., Santee, M. L., Schwartz, M. J., Wang, S., Fuller, R. A., Jarnot, R. F., Knosp, B. W., and Martinez, E.: Earth Observing System (EOS) Aura Microwave Limb Sounder (MLS) Version 4.2x Level 2 data quality and description document, Tech. Rep. D-33509 Rev. A, JPL, 2015.

Liu, H. L., Talaat, E. R., Roble, R. G., Lieberman, R. S., Riggin, D. M., and Yee, J. H.: The 6.5-day wave and its seasonal variability in the middle and upper atmosphere. Journal of Geophysical Research, 109, D21112. https://doi.org/10.1029/2004JD004795, 2004.

Liu, S.-M., Chen, Y.-H., Rao, J., Cao, C., Li, S.-Y., Ma, M.-H., and Wang, Y.-B.: Parallel Comparison of Major Sudden Stratospheric Warming Events in CESM1-WACCM and CESM2-WACCM. Atmosphere, 10, 679. https://doi.org/10.3390/atmos10110679, 2019.

Longuet-Higgins, M. S.: The eigenfunctions of Laplace's tidal equations over a sphere, Philosophical Transactions of the Royal Society of London. 262, 511-607. doi:10.1098/rsta.1968.0003, 1968.

Lu, X., Wu, H., Oberheide, J., Liu, H.-L., and McInerney, J. M.: Latitudinal double-peak structure of stationary planetary wave 1 in the austral winter middle atmosphere and its possible generation mechanism. Journal of Geophysical Research: Atmospheres, 123, 11,551–11,568. https://doi.org/10.1029/2018JD029172, 2018.

Ma, Z., Gong, Y., Zhang, S., Zhou, Q., Huang, C., Huang, K., Luo, J., Yu, Y., Li, G.: Study of a quasi-4-day oscillation during the 2018/2019 SSW over Mohe, China.

Journal of Geophysical Research: Space Physics, 125, e2019JA027687. https://doi.org/10.1029/2019JA027687, 2020.

Ma, Z., Gong, Y., Zhang, S., Xiao, Q., Xue, J., Huang, C., and Huang, K.: Understanding the excitation of quasi-6-day waves in both hemispheres during the September 2019 Antarctic SSW. Journal of Geophysical Research: Atmospheres, 127, e2021JD035984. https://doi.org/10.1029/2021JD035984, 2022.

Manney, G. L., Schwartz, M. J., Krüger, K., Santee, M. L., Pawson, S., Lee, J. N., Daffer, W. H., Fuller, R. A., and Livesey, N. J.: Aura Microwave Limb Sounder observations of dynamics and transport during the record breaking 2009 Arctic stratospheric major warming. Geophys. Res. Lett., 36(12), L12815. https://doi.org/10.1029/2009GL038586, 2009.

Matsuno, T.: A dynamical model of the stratospheric sudden warming. Journal of the Atmospheric Sciences, 28, 1479–1494. https://doi.org/10.1175/1520-0469(1971)028<1479:ADMOTS>2.0.CO;2, 1971.

Okui, H., Sato, K., Koshin, D., and Watanabe, S.: Formation of a mesospheric inversion layer and the subsequent elevated stratopause associated with the major stratospheric sudden warming in 2018/19. Journal of Geophysical Research: Atmospheres, 126, e2021JD034681. https://doi.org/10.1029/2021JD034681, 2021.

Pancheva, D., Mukhtarov, P., and Siskind, D. E.: The quasi-6-day waves in NOGAPS-ALPHA forecast model and their climatology in MLS/Aura measurements (2005-

2014), Journal of Atmospheric and Solar-Terrestrial Physics, 181, 19-37, https://doi.org/10.1016/j.jastp.2018.10.008, 2018.

Qin, Y., Gu, S-Y., Teng, C-K-M., Dou, X-K., Yu, Y., and Li, N.: Comprehensive study of the climatology of the quasi-6-day wave in the MLT region based on aura/MLS observations and SDWACCM-X simulations. Journal of Geophysical Research: Space Physics, 126, e2020JA028454. https://doi.org/10.1029/2020JA028454, 2021.

Rao, J., Ren, R., Chen, H., Liu, X., Yu, Y., Hu, J., and Zhou, Y.: Predictability of stratospheric sudden warmings in the Beijing Climate Center Forecast System with statistical error corrections. Journal of Geophysical Research: Atmospheres,124, 8385–8400. https://doi.org/10.1029/2019JD030900, 2019.

Rao, J., Garfinkel, C. I., and White, I. P.: Predicting the downward and surface influence of the February 2018 and January 2019 sudden stratospheric warming events in subseasonal to seasonal (S2S) models. Journal of Geophysical Research: Atmospheres, 125, e2019JD031919. https://doi.org/10.1029/2019JD031919, 2020.

Rao, J., Ren, R., Chen, H., Yu, Y., and Zhou, Y.: The stratospheric sudden warming event in February 2018 and its prediction by a climate system model. Journal of Geophysical Research: Atmospheres, 123, 13,332–13,345. https://doi.org/10.1029/2018JD028908, 2018.

Rao, J., Garfinkel, C. I., Wu, T., Lu, Y., Lu, Q., and Liang, Z.: The January 2021 sudden stratospheric warming and its prediction in subseasonal to seasonal models. Journal of Geophysical Research: Atmospheres, 126, e2021JD035057. https://doi.org/10.1029/2021JD035057, 2021.

Rhodes, C. T., Limpasuvan, V., and Orsolini, Y. J.: Eastward-propagating planetary waves prior to the january 2009 sudden stratospheric warming. Journal of Geophysical Research: Atmospheres, 126, e2020JD033696. https://doi.org/10.1029/2020JD033696, 2021.

Seviour, W. J. M., Mitchell, D. M., and Gray, L. J.: A practical method to identify displaced and split stratospheric polar vortex events. Geophys. Res. Lett., 40(19), 5268–5273. https://doi.org/10.1002/grl.50927, 2013.

Smith, A. K.: The origin of stationary planetary waves in the upper mesosphere. Journal of the Atmospheric Sciences, 60(24), 3033–3041. https://doi.org/10.1175/1520-0469(2003)060<3033:TOOSPW>2.0.CO;2, 2003.

Tunbridge, V. M., Sandford, D. J., and Mitchell, N. J.: Zonal wave numbers of the summertime 2 day planetary wave observed in the mesosphere by EOS Aura Microwave Limb Sounder, J. Geophys. Res., 116, D11103, doi:10.1029/2010JD014567, 2011.

Wang, J. C., Palo, S. E., Forbes, J. M., Marino, J., Moffat-Griffin, T., and Mitchell, N. J.: Unusual quasi 10-day planetary wave activity and the ionospheric response during the 2019 Southern Hemisphere sudden stratospheric warming. Journal of Geophysical Research: Space Physics, 126, e2021JA029286.

https://doi.org/10.1029/2021JA029286, 2021.

Wang, Y., Shulga, V., Milinevsky, G., Patoka, A., Evtushevsky, O., Klekociuk, A., Han, W., Grytsai, A., Shulga, D., Myshenko, V., and Antyufeyev, O.: Winter 2018 major sudden stratospheric warming impact on midlatitude mesosphere from microwave radiometer measurements, Atmos. Chem. Phys., 19, 10303–10317, https://doi.org/10.5194/acp-19-10303-2019, 2019.

White, I. P., Garfinkel, C. I., Cohen, J., Jucker, M., and Rao, J.: The impact of split and displacement sudden stratospheric warmings on the troposphere. Journal of Geophysical Research: Atmospheres, 126, e2020JD033989. https://doi.org/10.1029/2020JD033989, 2021.

Wright, C. J., Hall, R. J., Banyard, T. P., Hindley, N. P., Krisch, I., Mitchell, D. M., and Seviour, W. J. M.: Dynamical and surface impacts of the January 2021 sudden stratospheric warming in novel Aeolus wind observations, MLS and ERA5, Weather Clim. Dynam., 2, 1283–1301, https://doi.org/10.5194/wcd-2-1283-2021, 2021.

Wu, D. L., Hays, P. B., and Skinner, W. R.: A least-squares method for spectral-analysis of space-time series, J. Atmos. Sci., 52, 3501–3511, https://doi.org/10.1175/1520-0469(1995)052<3501:ALSMFS>2.0.CO;2, 1995.

Xiong, J., Wan, W., Ding, F., Liu, L., Hu, L., and Yan, C.: Two day wave traveling westward with wave number 1 during the sudden stratospheric warming in January 2017. Journal of Geophysical Research: Space Physics, 123, 3005–3013.

https://doi.org/10.1002/2017JA02517, 2018.

Xu, J., Smith, A. K., Wang, W., Jiang, G., Yuan, W., Gao, H., Yue, J., Funke, B., López-Puertas, M., Russell, I. I. I., and M, J.: An observational and theoretical study of the longitudinal variation in neutral temperature induced by aurora heating in the lower thermosphere. Journal of Geophysical Research: Space Physics, 118, 7410–7425, 2013.

Yamazaki, Y., and Matthias, V.: Large-amplitude quasi-10-day waves in the middle atmosphere during final warmings. Journal of Geophysical Research: Atmospheres, 124, 9874–9892. https://doi.org/10.1029/2019JD030634, 2019.

Yamazaki, Y., Matthias, V., Miyoshi, Y., Stolle, C., Siddiqui, T., Kervalishvili, G., Laštovička, J., Kozubek, M., Ward, W., Themens, D. R., Kristoffersen, S., Alken, P.: September 2019 Antarctic sudden stratospheric warming: Quasi-6-day wave burst and ionospheric effects. Geophysical Research Letters, 47, e2019GL086577. https://doi.org/10.1029/2019GL086577, 2020.

Yamazaki, Y., Matthias, V., and Miyoshi, Y.: Quasi-4-day wave: Atmospheric manifestation of the first symmetric Rossby normal mode of zonal wavenumber 2. Journal of Geophysical Research: Atmospheres, 126, e2021JD034855. https://doi.org/10.1029/2021JD034855, 2021.

Yu, F. R., Huang, K. M., Zhang, S. D., Huang, C. M., and Gong, Y.: Observations of eastward propagating quasi 6-day waves from the troposphere to the lower thermosphere during SSWs in early 2016. Journal of Geophysical Research:

Atmospheres, 127, e2021JD036017, https://doi.org/10.1029/2021JD036017, 2022.